Detonation loading of tubes in the modified shear wave speed regime

T. Chao and J. E. Shepherd

Graduate Aeronautical Laboratories, California Institute of Technology, Pasadena, CA 91125 USA

Abstract. We performed experiments and numerical simulations on a thin-wall aluminum tube with internal gaseous detonation loading in the modified shear wave speed regime. Strain gauges were used to determine the time-dependent hoop strain on the surface of the tube. The experimental results were compared with analytical models and numerical simulations with explicit finite element computation treating the detonation as a traveling load. Hoop strain amplification factors (defined as the ratio of the dynamic strain to the equivalent static strain) close to two were obtained both in the present experiments and simulations. No resonance phenomena in the hoop strain were found in either experiments or simulations. Computations reveal the existence of a resonance in the shear strain.

1 Introduction

As part of a study [1] on the failure of tubes due to internal explosions, we examined the elastic response of thin metal tubes loaded internally with an axially-propagating detonation wave. Previous studies [2–4] have shown that there are five critical wave speeds for which the linear response of one or more components of deformation becomes unbounded. Although it is well known [2,3] that resonance in the hoop strains exists at the first critical speed, no study in the literature was found on whether a similar resonance near the second critical speed will occur. The first two critical speeds are of engineering importance to metal tubes because the speeds of gaseous detonations are typically closer to the first two critical speeds than the third (bar) and fourth (dilatational) critical speeds. We examine one particular case in this note, the situation of an internal pressure load traveling near $v_{c1} = \sqrt{\kappa G/\rho}$, the second critical wave speed. This speed is also called the modified shear wave speed because of the application of the shell theory's shear correction factor, κ, to the shear speed of the material. According to the Tang [4] model, the steady-state solution does not exist at this speed.

Experiments and numerical simulations have been carried out with detonation wave speeds between 2187 m/s (above the first critical speed, v_{c0}, of the tube but below v_{c1}) and 3576 m/s (above v_{c1} but below the elastic bar wave speed, v_{c2}). These speeds were chosen to complement previous work [3] on the regime of speeds near v_{c0}. For the tube used in our study, the first four critical speeds are v_{c0}: 1013, v_{c1}: 2847, v_{c2}: 4982; v_{c3}: 5278 m/s and the material shear wave speed $c_s = 3055$ m/s for our specimens.

2 Experimental Setup

Figure 1 shows a schematic of the experimental setup which is described in detail by Chao [1]. Briefly, a detonation was produced in a 1.5 m long, thick-wall tube by acceleration of a flame initiated by a spark. The detonation then propagated into the 6061-T6 aluminum specimen tube which was 1.524 m long, 1.47 mm thick, and 41.28 mm outer diameter. The tubes were sealed at one end by a Teflon flange containing the spark plug, and the other end by a flange and an aluminum end plate. The pressure history of the detonation wave was measured by two piezo-electric pressure transducers. The pressure transducers were mounted 0.406 m apart in the detonation tube and arrival times of the wave fronts were

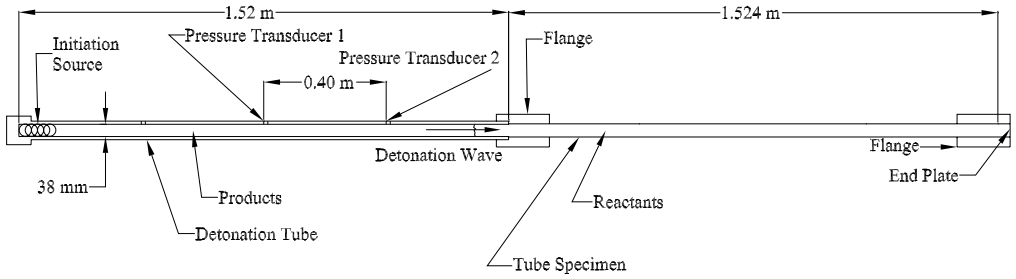

Fig. 1. Schematic of the tube assembly used for internal detonation loading of a tube specimen.

used to compute wave speeds. Five strain gauges were bonded to different locations on the external surface of the tubes to measure circumferential strain. The axial locations of the strain gauges measured from the left end of the specimen are SG1: 30.38 cm, SG2: 53.34 cm, SG3: 76.20 cm, SG4: 99.06 cm, SG5: 121.9 cm. The gauges were used in a Wheatstone bridge circuit and the output was conditioned by an amplifier with a bandwidth of 100 kHz.

A set of 15 stoichiometric hydrogen and oxygen mixtures was used with various amounts of dilution by either nitrogen or helium. These mixtures were chosen to vary the Chapman-Jouguet (CJ) detonation velocity without significantly altering the CJ pressure. The initial pressure for all cases was 0.1 MPa and the detonation velocity ranged from 2200 to 2800 m/s for the nitrogen cases and from 2900 to 3600 m/s for the helium cases.

3 Finite-Element Simulations

Finite-element simulations were performed to complement every experiment. The specimen tube was modeled with axisymmetric solid elements using the commercial explicit finite-element code LS-Dyna V.960. Full integration was used but to decrease computational costs, only 35.56 cm of the tube was modeled. The left end of the tube was simply supported radially but not axially. Twenty elements were used in the radial direction and 5039 elements in the axial direction. The whole model had 100780 elements. The choice of the number of elements was made after a trial-and-error process at resolving the high-frequency shear stresses.

The location for recording stresses was at 12.7 cm from the left end and in the middle of the wall thickness. The location for recording radial displacements was at 12.7 cm from the left end and on the outside diameter of the wall. The choice of 12.7 cm avoided contamination by reflected dilatational waves and eliminated the influence of boundary conditions from the right end throughout the duration of the simulation.

The traveling pressure load model was modeled as in Beltman and Shepherd [3]. The load was prescribed as a function of time at each node. The force history was a discrete version of the exponential approximation to the Taylor-Zeldovich model and the parameters were obtained by curve-fitting the pressure trace from the second transducer. The exponential decay from the CJ point was approximated by 5039 linear segments over 0.11 ms, which was the duration of the simulations.

Very high spatial and temporal resolution is required to simulate shear waves in a thin tube. Considering wave propagation in the thickness direction, we estimate that the traveling load can excite shear wave oscillations with a frequency up to 3 MHz, a factor of 100 higher than observed by flexural waves. An upper bound of the mesh size could be estimated using the flexural wavelength. Flexural waves for these experiments ranged from 37 to 40 kHz, with wavelengths from 55 to 97 mm. Since the wavelength was much larger than the wall thickness of 1.5 mm, as long as the mesh size was smaller than the wall thickness, flexural waves could be more than adequately resolved. Note that since

the flexural wavelengths were also much larger than the length of the strain gauges (0.81 mm), the experimental hoop strains were also adequately resolved.

It was found after several trials that considerations of flexural wavelengths and detonation cell sizes were insufficient in resolving transverse shear because higher-frequency components were being discovered as the mesh size went down and sampling rate went up. At a mesh size of 71 μm (axial) by 74 μm (radial) and a sampling rate of 91 MHz, the shear stress traces appeared to have converged, although a rigorous convergence study was not attempted. At this spatial and temporal resolution, we observed transverse shear waves with frequency components up to 3.3 MHz traveling at a speed of 3576 m/s (highest in this study) with 15 elements per wavelength and a time step of 10 ns.

4 Results and Discussion

4.1 Hoop Strain

Hoop strain amplification factors (defined as the ratio of the maximum dynamic hoop strain to the equivalent static hoop strain) close to two were obtained both in the present experiments and simulations. No resonance phenomena in the hoop strain were found near the modified shear wave speed such as observed in previous studies [2,3] for the flexural wave resonance ($U_{cj} \sim v_{c0}$) regime. This is consistent with the analytical model [4] of linear elastic tubes under internal traveling load. Figure 2 shows a comparison between the experimental, numerical, and analytical hoop strain dynamic amplification factor. The maximum difference between experiment and simulation was about 24%. On the other hand, the analytical model differed from the experimental values by as much as 42%. This larger difference may be due to the approximating assumptions of the shell theory used in the analytical model. The finite-element model gave results closer to measurements because it used solid elements instead of shell elements and included transient effects. Moreover, both theory and simulations overestimated the hoop strains; no material damping effects were included in these calculations.

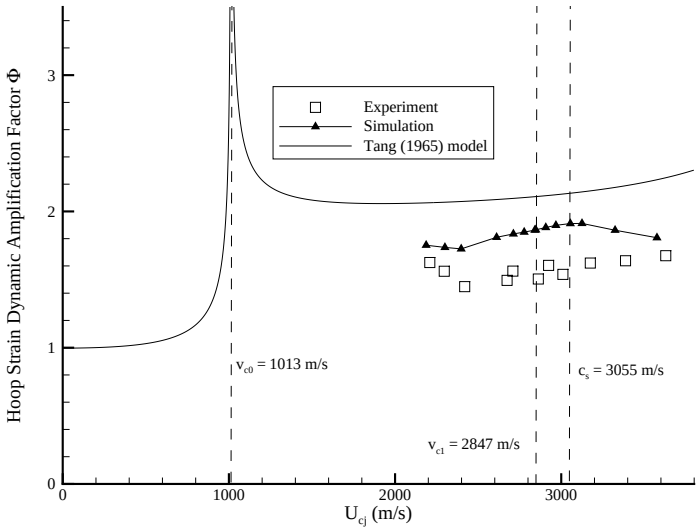

Fig. 2. Dynamic amplification factor for hoop strain.

Figure 3 shows a typical set of measured hoop strain and pressure traces. For this experiment, the CJ speed was 2841 m/s. Although this was very close to the theoretical

modified shear wave speed of 2847 m/s, the characteristic behavior of the oscillatory strains did not differ qualitatively from the measured strains for the other wave speeds tested. Figure 4 shows a comparison between measurement and simulation.

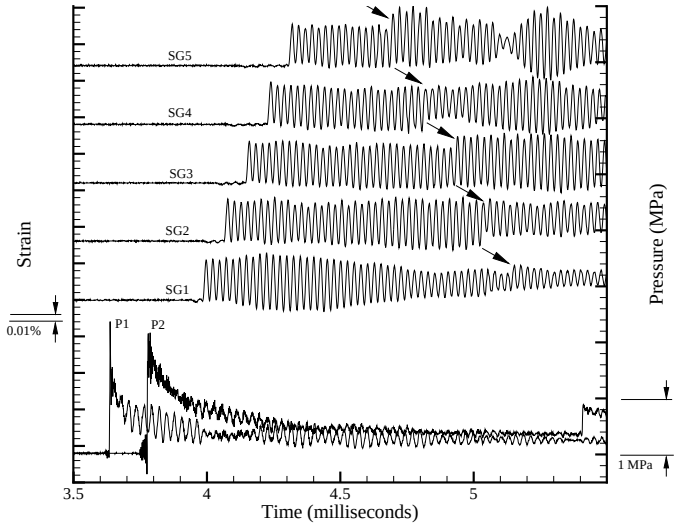

Fig. 3. Experimental hoop strain and pressure histories for Shot 41, $U_{cj} = 2841$ m/s. Arrows indicate arrival of the shock wave reflected from the end plate. The maximum strain plotted in Fig. 2 was determined from the portion of the signal prior to the arrival of the shock wave.

4.2 Transverse Shear Stress

Computed transverse shear stresses, on the other hand, showed drastically different behavior as the detonation wave speed U_{cj} was varied across the range containing v_{c1}. Since there was no known way of directly measuring transverse shear stress and also no known theoretical solution of transverse shear stresses under these loading conditions, only numerical data were available.

The maximum frequencies of these shear stresses were two orders of magnitude higher than those for the hoop strains. Three kinds of behavior can be distinguished from the traces in Fig. 5. CJ speeds below that of 2777 m/s (6th trace from bottom) can be classified into the first type, those between 2777 m/s and 2847 m/s (8th trace from bottom) into the second type, and those above 3125 m/s (top three traces) into the third type. The first and second types had bulk shear disturbances ahead of the traveling load (the circle denotes coincidence with the detonation wave front). The second type is characterized by a spike in shear stress which traveled with the detonation front, whereas in the first type, the tail of the bulk shear disturbance coincided with the detonation front. No bulk shear disturbance was observed to travel faster than c_s, the material shear wave speed, for type one and type two. The arrival time for the waves associated with c_s was 0.0416 ms. When the detonation wave speed was above c_s, corresponding to type three, the front of the shear disturbance traveled with the detonation front.

The dynamic shear amplification factor, Φ_s, is shown in Fig. 6. The value of Φ_s starts from about 2 for $U_{cj} = 2200$ m/s, rises to a maximum value of about 4.5 at about 2777 m/s, and drops to about 0.3 at 3600 m/s. The maximum amplification is observed at a speed that is 3% lower than the computed [4] second critical speed.

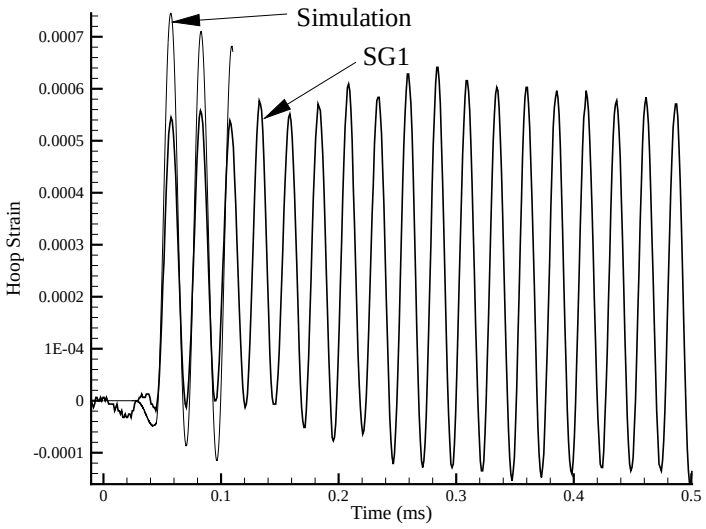

Fig. 4. Comparison between simulation and experiment for Shot 41, U_{cj} = 2841 m/s. SG1 is plotted here because it was closest among all the strain gauges to the recording location in the simulation. Simulation terminated at 0.11 ms. SG1 has been time-shifted so that the flexural wave front coincides with the simulated flexural wave front for comparison.

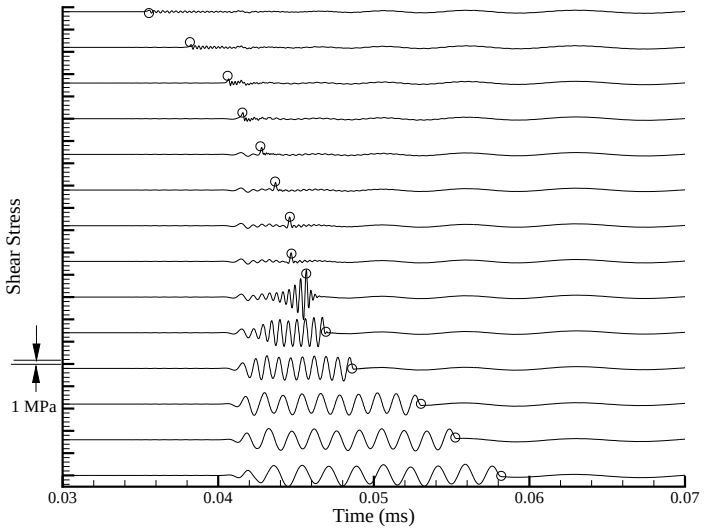

Fig. 5. Computed transverse shear stress for detonation wave speeds between 2200 m/s to 3600 m/s, increasing from bottom to top. Circles denote the detonation wave front.

5 Conclusions

It was found that there is no resonance in hoop strain at the second critical speed. This was verified experimentally and it also agrees with the analytical model [4]. It was found that there was a resonance in the shear strain at the second critical speed. Computed transverse shear strains reached 4.5 times that of the static equivalent transverse shear

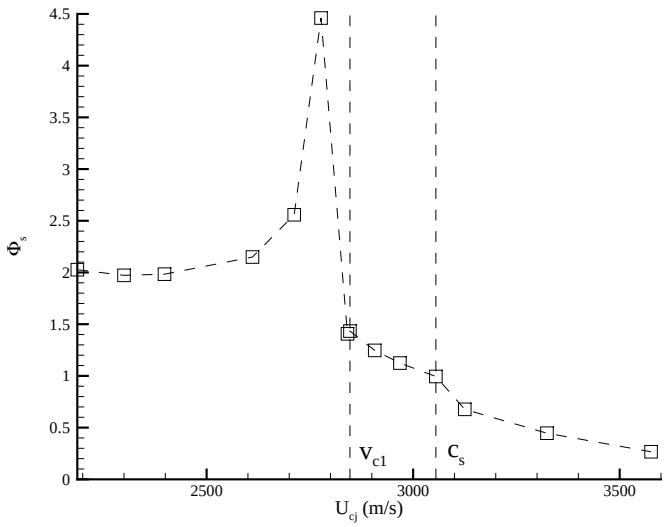

Fig. 6. Shear amplification factor near the modified shear wave speed.

strains. Since transverse shear stresses are small compared to hoop stresses (for example, the highest computed shear stress was 6 MPa compared to the maximum hoop stress of 49 MPa), it is unlikely that plain tubes will fail in shear due to shear resonance. However, for tubes with shear stress concentrators such as joints, elbows, notches, surface cracks, and interfacial cracks, transverse shear amplification may play a role in design and failure analyses.

Acknowledgement

We thank Prof. W. G. Knauss and Prof. G. Ravichandran for their advice and technical assistance in this project. This work was supported by the Center for Simulation of Dynamic Response of Materials at Caltech, sponsored by the US Department of Energy.

References

1. Tong Wa Chao. *Gaseous Detonation-Driven Fracture of Tubes*. PhD thesis, California Institute of Technology, Pasadena, California, March 2004.
2. W.M. Beltman, E.N. Burcsu, J.E. Shepherd, and L. Zuhal. The structural response of cylindrical shells to internal shock loading. *Journal of Pressure Vessel Technology*, 121:315–322, 1999.
3. W.M. Beltman and J.E. Shepherd. Linear elastic response of tubes to internal detonation loading. *Journal of Sound and Vibration*, 252(4):617–655, 2002.
4. S. Tang. Dynamic response of a tube under moving pressure. In *Proceedings of the American Society of Civil Engineers*, volume 5, pages 97–122. Engineering Mechanics Division, October 1965.